Pertanika J. Sci. & Technol. 32 (6): 2405 - 2420 (2024)

PERTANIKA JOURNALS

SCIENCE & TECHNOLOGY

Journal homepage: http://www.pertanika.upm.edu.my/

Performance Comparison of Seed Generation Techniques of Stimulated Brillouin Scattering-based Microwave Photonics Amplifier and Filter

Shahad Khudhair Abbas[1], Noran Azizan Cholan[2], Mohd Saiful Dzulkefly Zan[3], Mohd Adzir Mahdi[1,4], Makhfudzah Mokhtar[1,4] and Zuraidah Zan[1,4]*

[1]Department of Computer and Communication Systems Engineering, Faculty of Engineering, Universiti Putra Malaysia, 43400 Serdang, Selangor, Malaysia
[2]Faculty of Electrical and Electronics Engineering, Universiti Tun Hussein Onn Malaysia (UTHM), 86400 Parit Raja, Batu Pahat, Johor, Malaysia
[3]Department of Electrical, Electronic & Systems Engineering, Faculty of Engineering & Built Environment, Universiti Kebangsaan Malaysia, Selangor 43600, Malaysia
[4]Wireless and Photonics Networks (WiPNET) Research Center, Faculty of Engineering, Universiti Putra Malaysia,43400 Serdang, Selangor, Malaysia

ABSTRACT

This work presents a Brillouin amplification performance comparison of seed generation techniques using double-sideband suppressed carrier (DSB-SC) and single-sideband suppressed carrier (SSB-SC) modulations. The SSB-SC is obtained using an optical bandpass filter (OBPF) and in-phase and quadrature Mach-Zehnder modulator (IQ-MZM). All three techniques provide high amplification performance with optical signal-to-noise ratio (OSNR) enhancement of 37.47 dB, 33.14 dB, and 32.67 dB using DSB-SC, SSB-SC/OBPF, and SSB-SC/IQ-MZM, respectively. The best seed generation technique is using the DSB with a signal amplification of 62.47 dB. The technique presents ~4 dB higher OSNR enhancement due to the dual-energy transfer obtained from the beating process of the DSB than SSB. A ~3 dB OSNR reduction is found when pump linewidth (LW) was changed from 1kHz to 50 MHz, which suggests using a low-cost pump source whenever the OSNR reduction is not critical. The work also shows that the three techniques required 10 dBm stimulated Brillouin scattering threshold (SBST) to stimulate the process. An additional analysis of DSB-SC shows that a high-carrier suppression during the

ARTICLE INFO

Article history:
Received: 29 August 2023
Accepted: 25 March 2024
Published: 09 October 2024

DOI: https://doi.org/10.47836/pjst.32.6.01

E-mail addresses:
shahadkhudhair92@gmail.com (Shahad Khudair Abbas)
noran@uthm.edu.my (Noran Azizan Cholan)
saifuldzul@ukm.edu.my (Mohd Saiful Dzulkefly Zan)
mam@upm.edu.my (Mohd Adzir Mahdi)
fudzah@upm.edu.my (Makhfudzah Mokhtar)
zuraidahz@upm.edu.my (Zuraidah Zan)
* Corresponding author

ISSN: 0128-7680
e-ISSN: 2231-8526

seed generation technique using MZMs is insignificant to the amplification performance. The high-carrier suppression produces a high seed signal power that distorts the Brillouin gain spectrum (BGS) and the pump depletion region, hence reducing the Brillouin gain (BG). Since carrier suppression is not a primary consideration, a cost-effective MZM with a modest extinction ratio requirement is allowed. The relaxed requirement of the pump's linewidth and MZM's extinction ratio suggest a cost-effective development of the SBS-based optical amplifier with narrow filter bandwidth.

Keywords: Brillouin amplifier, double-sideband, noise ratio enhancement, optical signal, single-sideband

INTRODUCTION

Microwave photonic filters based on stimulated Brillouin scattering (SBS) have become a promising alternative for ultra-narrow passband filters with noise suppression and amplification within the filter bandwidth (Pang et al., 2022; Zhang et al., 2022). With the SBS-based amplification, a narrow gain bandwidth between 10 to 100 MHz can be obtained with a lower pump power than using a Raman-based (Qi et al., 2022). The pump operated at a specific power is required to reach a Brillouin threshold and produce an SBS process where most of the incident power is reflected and produces an amplification. A Stokes signal at around 11 GHz from the laser pump's center frequency is obtained with more than 20-dB Brillouin gain (BG) at the pump power that exceeds the SBS threshold (SBST). SBS is known for its amplification with a high selectivity filtering owing to its high selectivity amplification and becomes a promising approach to enhancing a transmission system's optical signal-to-noise ratio (OSNR).

In Marhic and Cholan (2014), signal amplification with a narrow bandwidth was shown to provide noise suppression with 27-dB OSNR enhancement. It is supported by Nieves et al. (2021), where noise suppression can be obtained with combinations of waveguide properties, pump power, Stokes field, pulse durations, and interaction time. The SBS-based amplification needs a frequency-locking or beating between the optical signal (required to be amplified) with the backward-generated Stokes within a Brillouin-gain-bandwidth (BGBW). The signal required to be amplified is a probe or seed signal in the SBS-based amplification. Techniques to generate and beat the seed signal with Brillouin's Stokes can be done using a single or two independent laser pumps (Gertler et al., 2022; Marhic & Cholan, 2014).

A recent study utilizing two laser pumps was presented by Gertler et al. (2022) with two free-running laser sources around 1550 nm wavelength with a narrow linewidth (LW). In this study, the seed generation was done using two laser pumps to modulate the intensity of a wideband RF signal and produce a double sideband-suppressed carrier (DSB-SC) of several RF tones with a fully suppressed carrier (Ali et al., 2022; Gertler et

al., 2022). It requires a special device, a multi-port photonic-phononic emitter-receiver (PPER), fabricated using phononic crystals. The seed generation was done within these special waveguides that can generate and tune the seed at the expense of complexity and implementation costs. Another study reported using a single laser as the pump source but, however, required three phase-modulators for the seed generations using DSB, where at the final stage of the generation, the optical carrier was also suppressed using an optical filter (Du et al., 2023). The study focused on beating the generated seeds for the application of spectral measurement without emphasizing the modulation techniques used. Meanwhile, a study utilizing a single sideband modulation with the suppressed carrier (SSB-SC), which utilized the SBS effect in fiber to obtain the gain spectrum, was reported by Bhogal and Sindhwani (2022). The study, however, focuses on frequency shifting and a high carrier suppressed with the effect of Brillouin gain. In Marhic and Cholan (2014), an SBS experiment demonstrated 27-dB OSNR signal enhancement using a continuous-wave pump. A narrow linewidth (LW) laser pump with 30 dBm output power has been used with an intensity modulator focusing on a DSB modulation for the seed signal generation. The work has yet to explain the condition of the seed signal generation in terms of its modulation type, carrier suppression requirement, pump power, and interaction within a BGBW.

In this manuscript, the performance of the seed generation techniques comparing the DSB and SSB modulations is presented to obtain a high-gain SBS-based amplifier with a narrow band associated with the Brillouin gain bandwidth. Typical DSB modulation with carrier suppression adjusted using voltage biasing is obtained using a single-armed Mach Zehnder modulator (MZM), while two techniques are used for the SSB modulation. The first one is done by adding an optical bandpass (OBP) filter to remove an upper sideband, and the second is utilizing a costly optical modulator to generate the SSB directly after the modulator's output with the use of in-phase and quadrature MZM (IQ-MZM). The carrier suppression is also tuned with the biasing voltage supplied to the MZM's arms without any biasing control circuit. The proposed setups are more straightforward and cost-effective than the technique used by Gertler et al. (2022) and Ali et al. (2022), which requires a PPER device to perform sideband filtering and carrier suppression.

On the other hand, Du et al. (2023) performed the SBS generation using the DSB modulation but with cascaded phase modulations (PM) and OBP filters. Two free-running laser diodes and optical modulators were utilized by Ali et al. (2022) to perform the microwave filtering based on SBS, which again incurred additional cost and phase noise due to the free-running lasers, as opposed to a single laser diode with single MZM to perform the SBS seed generations in our proposed work. The single laser diode produces a strong phase correlation between the laser and the generated seed, reducing the phase noise impact on the system (Mandalawi et al., 2019). The work also highlights the requirement of the suppressed carrier for the modulation, which can be used to identify the MZM

specifications, specifically the required extinction ratio. With the narrow bandwidth, a high selectivity of 50 MHz optical bandwidth can be obtained with a high OSNR, indicating noise suppression. It can be another option for a high selectivity optical amplification as opposed to the typical Erbium-doped fiber-based amplifier with a wide bandwidth of 35 nm where a predominant amplified spontaneous emission (ASE) noise is imposed within the amplified signal. Investigations have been carried out in this work using VPItransmissionMaker™, a well-known simulator that industries and academics use to mimic expensive optical systems. The performance comparison between the SBS and DSB modulations shows that DSB provides the best seed generation technique to obtain a high gain. OSNR is the DSB modulation technique with a relaxed carrier suppression requirement. The technique provides a signal amplification of 62.47 dB with an OSNR enhancement of 37.47 dB. The results suggested using a cost-effective MZM with a modest extinction ratio requirement.

METHODOLOGY

Seed Generation Techniques

A single pump source at a frequency, f_o, generates the seed signal and the SBS process. The pump signal, f_o, is amplified by an erbium-doped fiber amplifier (EDFA) to satisfy the SBST required to stimulate the Brillouin process and generate BGBW. Figure 1 illustrates the spectrum modulation and its interaction with BG and BGBW.

The induced soundwave signal has an acoustic velocity, V_a, to generate the Stokes signal at a BFS of v_B given by $v_B = \frac{2nV_a}{\lambda}$, where n is the optical fiber refractive index, and λ is the pump-signal wavelength (Ali et al., 2022; Du et al., 2023). The signal that must be enhanced or amplified needs to be injected with the same frequency and direction of the BFS aligned within the BGBW. In this case, a seed signal is backward injected into the optical fiber, beaten with the pump signal, and an amplified signal is produced at $-f_m$. The pump signal, f_o, is modulated with an RF signal, f_m, tuned to v_B, as shown in Figure 1(b). The MZM is DC-biased at a null point with respect to the MZM's transfer function, as shown in Figure 1(b)(iii); according to Figure 1(b)(i), the generation of the SSB-SC seed signal using an OBPF after the MZM lets the lower-sideband signal interact within BGBW and filter out the upper-sideband. Meanwhile, Figure 1(b)(ii) shows the SSB-SC seed signal generated using an IQ-MZM. This technique requires a local oscillator tuned to f_m where one of the RF signals is 90° phase-shifted from the other inputs to produce in-phase and quadrature RF signal components. These signals drive the IQ-MZM to produce a seed signal at v_B. The IQ-MZM is biased at the quadrature point of the transfer function, as illustrated in Figure 1(b)(iii). The theoretical mathematical models to explain Brillouin's Stokes amplification and the seed generations have been reported by Gökhan et al. (2018), Loayssa et al. (2004) and Qing et al. (2016).

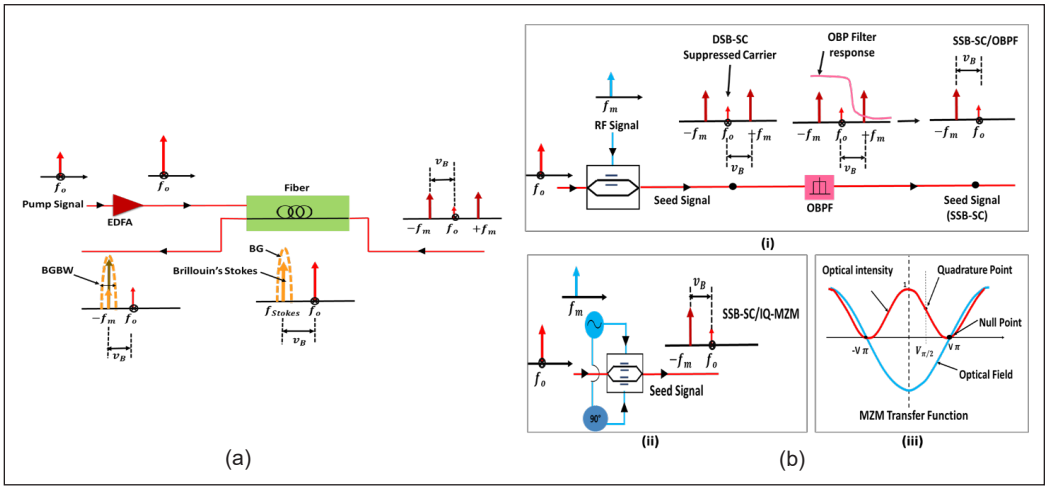

Figure 1. Illustration of (a) Brillouin's Stokes with BG generation and seed interaction within BGBW and (b) seed signal generations using MZMs to generate (i) DSB-SC and SSB-SC using an optical bandpass filter (OBPF), (ii) SSB-SC using in-phase and quadrature Mach-Zehnder modulator (IQ-MZM) with biasing voltages with respect to (iii) MZM's transfer function

Simulation Setup

The simulation setup of SBS-based optical amplification with signals before the interaction/beating processes using (a) DSB-SC, (b) SSB- SC/OBPF, and (c) SSB-SC/IQ-MZM of seed signal generation blocks illustrated by the inset diagrams of Figure 2. A CW-laser with a center frequency of 193.1 THz (corresponding to 1552.52 nm of wavelength), an output power of 6 dBm, and a linewidth (LW) of 1 MHz is used as the pump source for this system. The CW-laser light is split by 50/50 Coupler 2, and the outputs are used for the pump source and to drive the MZM denoted as a carrier signal in the seed generation block. The MZM is used to generate the BFS light, in which an RF signal generator tunes the amount of the frequency shift. The optical MZM's extinction ratio is set to a typical value of 30 dB for all configurations, indicating the MZM's carrier-suppression ratio. The carrier suppression is obtained by biasing the MZM near the null region of its transfer function curve.

The output light of the CW-laser is added with an amplified-spontaneous emission (ASE) noise source to provide a constant white noise and a gain-controlled EDFA to vary the level of a noise- floor for OSNR and gain analyses. The combined CW-light and the ASE noise signal are fed onto an OBPF with a rectangular transfer function to limit the signal bandwidth (BW). At Point 1, the CW-light power is maintained at 3 dBm with an OSNR of 25 dB. The pump source at Output 1 of Coupler 2 is amplified to 30 dBm using a power-controlled EDFA and connected to a polarization controller (PC1) before the light is injected into a bidirectional optical fiber to stimulate a Brillouin process. PC1 is

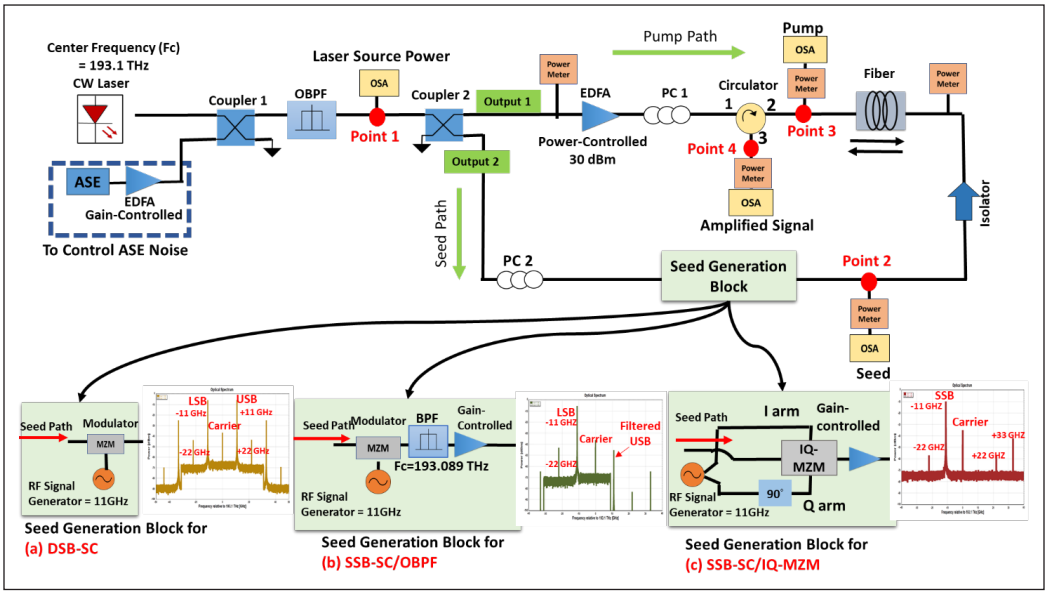

Figure 2. Simulation setups of SBS-based optical amplification using (a) DSB-SC, (b) SSB-SC/OBPF and (c) SSB-SC/IQ-MZM seed generation blocks

required before the fiber because the EDFA changes the signal's state of polarization (Ali et al., 2023; Du et al., 2023).

The fiber parameters set are 14 km in length, 0.2 dB/km of attenuation, effective core area, A_{eff} of 8×10^{-10} m^2, Brillouin gain coefficient, g_o of 4.6×10^{-11} m/W, intrinsic Brillouin bandwidth (BBW) of 50 MHz, Brillouin frequency shift, v_B 11 GHz, and a nonlinear index of 26×10^{-21} m^2/W. The CW-light at Output, 2 of Coupler 2, is linearly polarized before it is used to drive the MZM in the seed generation block. The pump and seed signals must be polarized because the SBS is a polarizer-dependence process (Deventer & Boot, 1994). The respective modulation techniques of DSB-SC, SSB-SC/OBPF and SSB-SC/IQ-MZM are shown in the inset diagrams of Figure 2(a), (b) and (c), respectively.

Every modulation technique is modulated with an RF signal from a local oscillator to generate side tones at a frequency equal to v_B. The DSB-SC is constructed using a single RF-drive MZM with the biasing voltage set to 1 V to obtain carrier suppression. A complete null carrier- suppression cannot be obtained with the supplied biasing voltage due to the low 30-dB extinction ratio of the MZM. Thus, a carrier leakage of 3 dB, shown by the inset spectrum of Figure 2(a), is produced. The modulated signal also produced harmonic components at ± 22 and ±33 GHz. The SSB-SC/OBPF technique is the same as the DSB-SC design but uses an OBPF of 60 GHz BW, 40 dB stop-band centered at 193.089 THz with a rectangular transfer function. It filters out the USB and passes the LSB part of the seed signal. The LSB at 193.089 THz is obtained with respect to the difference between the center frequency, f_o and v_B. The seed signal spectrum of the SSB-SC/OBPF with 3-dB

carrier leakage and the harmonic component at -22 GHz can be shown in Figure 2(b). Figure 2(c) shows the SSB-SC/IQ-MZM design, constructed using an IQ-MZM with an RF signal generator connected to a power splitter to provide the in-phase signal. In contrast, the quadrature signal component is produced after the 90^0-phase shift. The I- and Q-arms are biased at 0.5 V. The output signal is the SSB at v_B with 4 dB carrier leakage, and 23.3-dB carrier suppression is obtained with the harmonic components at ± 22 and +33 GHz. The seed signal power at Point 2 is -2 dBm for the three designs. The insertion losses of the components used in the SSB-SC/OBPF and SSB-SC/IQ- MZM seed generation block are compensated using an EDFA. The output of the seed generation block is injected through an isolator to prevent a back-reflection, fed into the bidirectional universal fiber and then extracted through Port 3 of the circulator as the amplified signal denoted as Point 4.

RESULTS AND DISCUSSION

SBS-based signal amplification is taken at Point 4 of the circulator's output. The spectra are analyzed to identify the gain and the OSNR enhancement obtained by comparing the SBS amplified signal to the pump source at the output at Point 1 of Figure 3.

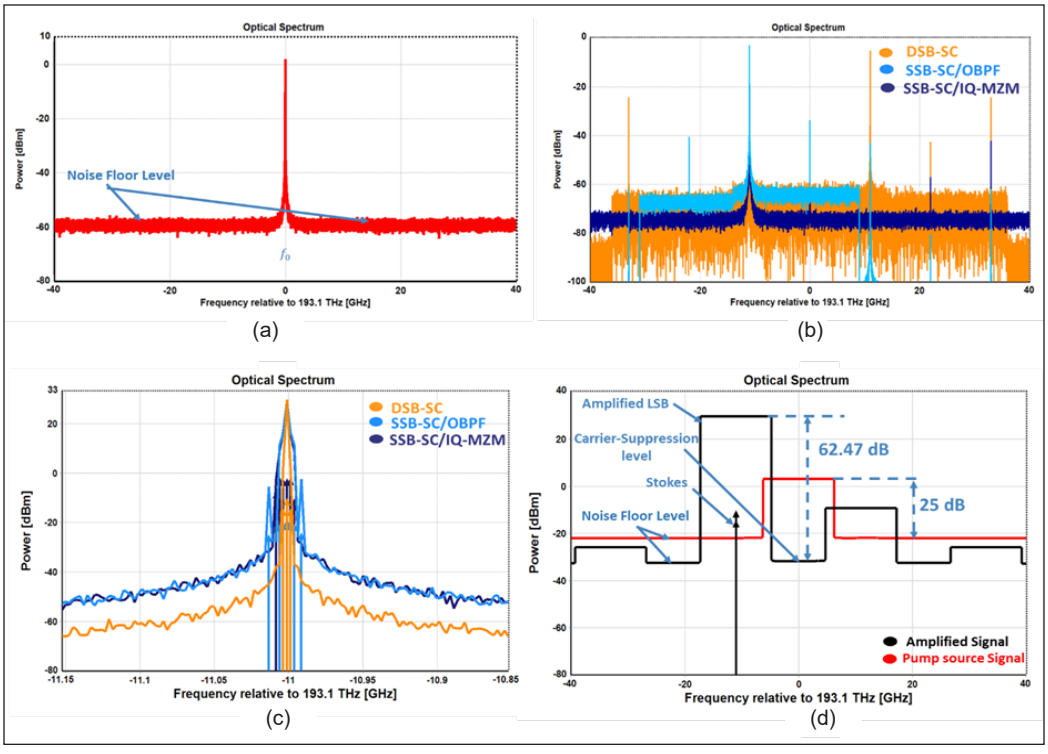

Figure 3. Spectra of (a) laser source signal at Point 1, (b) seed signal generation before the interaction at Point 2 for DSB-SC, SSB-SC/OBPF and SSB-SC/IQ-MZM, (c) aligned Stokes with the amplified signals of DSB-SC and SSB-SC at 2 MHz resolution bandwidth (RBW) and (d) amplified signal at Point 4 using DSB-SC seed generation with its pump source signal at Point 1 with RBW of 12.5 GHz

The 0.1 nm RBW is a standard OSNR measurement using a typical OSA (Ali et al., 2022). The spectrum has been magnified from a Lorentzian-shaped spectrum to present the Stokes signal at -11 GHz, where the simulator represents the Stokes signal using the arrows. The Stokes produces a Lorentzian-shaped BG with a narrow BGBW, whereas the gain will amplify the seed signal injected backward within the interaction area. In contrast, the signal and noise outside the BGBW are not affected. It produced a much narrower amplifier BW than an EDFA, amplified all the signals within a wide BW, and added an ASE noise onto the amplified signal (Ali et al., 2022). The Stokes signal is produced when part of the pump signal is back-scattered due to the periodical modulation of the refractive index when it interacts with the fiber medium. Stokes signal is considered a noise if there is no backward seed signal. The refractive index modulation obtains an exponentially increased back-scattered pump power signal, similar to a Bragg condition. The power is then transferred to the seed signal and amplified (Ali et al., 2022).

The Stokes wave power is higher in the DSB-SC than in the SSB-SCs due to the higher transferred power of the DSB to the pump, which leads to a more back-scattered pump power (Ali et al., 2022; Preussler & Schneider, 2015). The measurement of the OSNR enhancement is shown by taking the difference between the OSNR of the amplified signal with respect to its noise floor (black line) and the pump source signal with its respective noise floor (red line), as shown in Figure 3(d) (Marhic & Cholan, 2014). The noise floor of the amplified signal is represented by the carrier-suppression level of the seed generation technique, which is, in this case, the DSB-SC. The OSNR enhancement obtained is 37.47 dB, resulting from the subtraction between 62.47 dB and 25 dB, as shown in Figure 3(d).

Figure 4(a) shows the harmonic frequency components at multiple $\pm f_m$ for the DSB-SC and at multiple $-f_m$ for the SSB-SC from the laser pump's center frequency at 193.089 THz, where each component is separated at v_B of 11 GHz. When the Stokes signal is aligned, the LSB signal at -11 GHz away from the laser pump's center frequency is amplified to a peak power of 30 dBm. When the LSB frequency does not match the BFS, no power transfer process between the seed and pump signals will occur. These indicate that the signals are unaligned; hence, the seed signal (LSB) will not be amplified. In this simulation, the Stokes signal is fixed to v_B with a constant phase. The pump power used is 30 dBm. The OSNRs are 62.47 dB, 58.14 dB and 57.67 dB for the DSB-SC, SSB-SC/OBPF, and SSB-SC/IQ-MZM seed generation techniques, respectively. Measured BGs with respect to the unamplified (unaligned seed signal within BGBW) are 38.4 dB, 34.08 dB and 33.6 dB for the DSB-SC, SSB-SC/OBPF and SSB-SC/IQ-MZM, respectively.

A BGBW is obtained by taking a full-wave half maximum (FWHM) measurement of the amplified spectrum. The amplified optical power obtained at Point 4 is similar to the pump power at Point 3 due to the total power reflection from the saturated pump signal (Aoki et al., 1988; Ravet et al., 2008). The obtained OSNR enhancements of 37.47 dB,

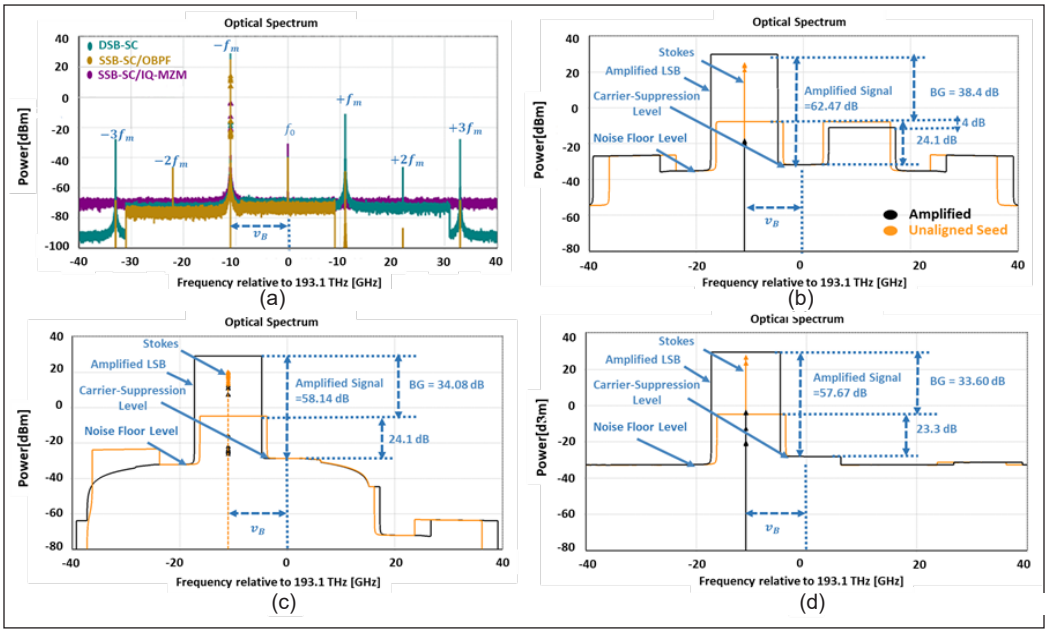

Figure 4. Spectra of the aligned and unaligned seed with Stokes signals obtained at Point 4 for (a) all seed generation techniques at 2 MHz RBW, (b) DSB-SC, (c) SSB-SC/OBPF and (d) SSB-SC/IQ-MZM seed generation techniques at 12.5 GHz RBW

33.14 dB and 32.67 dB for the DSB-SC, SSB-SC/OBPF and SSB-SC/IQ-MZM seed signal generation techniques, respectively. 4-dB higher OSNR enhancement is obtained using the DSB- SC than the SSB-SCs due to the higher power transferred from the USB at $+f_m$ and carrier at f_o to the LSB at $-f_m$. It is shown in Figure 4(b), where the amplified USB power (black line) is reduced by 4 dB compared to the unamplified USB (orange line) when no alignment occurred. It confirmed the result obtained in Marhic & Cholan (2014) with slightly higher OSNR enhancement due to the circulator's low insertion loss and high isolation.

Figure 5 analyzes the noise power level before and after the interaction and shows additional noise from the Brillouin amplifier. The DSB-SC amplification signal is compared since the noise floor level is identical to the SSB-SCs. It shows a ~ 24 dB additional noise power compared to the pump source signal. It is due to the characteristic of EDFA that amplifies the whole signal band, including the noise. The amplified signal noise level decreased by 9 dB due to component power loss (coupler, polarizer and MZM). Hence, the Brillouin amplifier added negligible noise to the signal, in agreement with Souidi et al. (2016). The Brillouin amplifier added low noise compared to EDFA due to Brillouin's narrow gain bandwidth.

In this simulation, the injected seed signal power into the fiber is fixed at -2 dBm to compare the seed generation techniques. The Stokes signal peak power is obtained by the

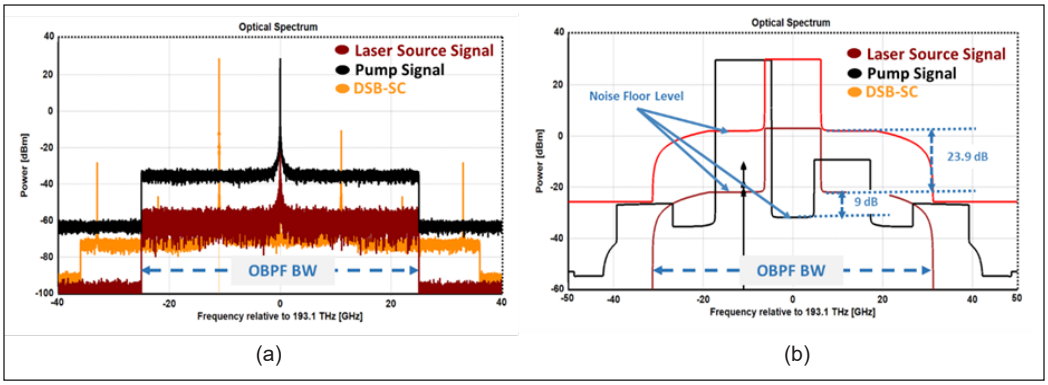

Figure 5. Spectra of the laser source signal, Pump signal, and amplified signal of DSB-SC at (a) 2 MHz RBW and (b) 12.5 GHz RBW

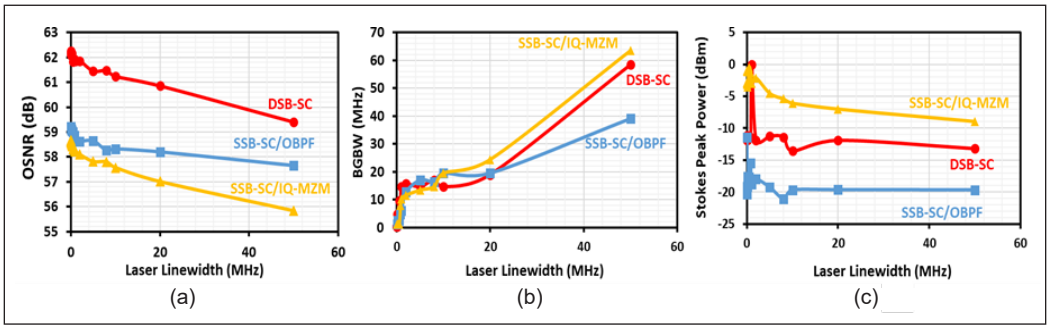

Figure 6. Pump source phase noise effect to (a) amplified signal OSNR, (b) BGBW and (c) Stokes's peak power using DSB-SC, SSB-SC/OBPF and SSB-SC/IQ-MZM seed generation techniques

highest arrow peak power value, which indicates the Stokes signal. Figure 6(a) shows that the highest OSNR is obtained with the narrowest LW and fluctuates when the LW is broadened for the three modulations. It is expected that the pump LW is narrower than the intrinsic Brillouin bandwidth. All three seed generation techniques require a coherence source for the highest amplification. When the pump source with a high phase noise or an insufficient coherence pump source is used, the phase noise becomes the dominant factor that reduces the obtained gain and induces the Brillouin gain fluctuations. It can be associated with the obtained fluctuated OSNR when the LW is broadened. However, the fluctuations amount is negligible and considered stable due to the frequency-locking approach that makes the generated Stokes wave follow the pump signal frequency, consequently canceling gain fluctuations and providing a stable amplification as explained in Figure 6(a) (Souidi et al., 2016).

The results agreed well with the BGBW, as shown in Figure 6(b). To obtain the maximum gain, the pump LW must be much narrower than the intrinsic Brillouin bandwidth of 50 MHz in the simulation setup. The BGBW is relatively broadened and fluctuates

when the pump LW is increased, which agrees with its respective amount of gain shown in Figure 6(a). The broadened pump LW also affects the threshold power required to produce the stimulated Brillouin effect. Consequently, reducing the SBST will reduce the gain amplification produced by the SBS (Ali et al., 2022; Du et al., 2023; Harish & Nilsson, 2019). Figure 6(c) shows that the narrower the pump LW than the Brillouin bandwidth, the stronger the Stokes signal is obtained, resulting in the highest gain. Figure 6 shows that the DSB-SC provides better overall performance than the SSB-SC/IQ-MZM and SSB-SC/OBPF due to the double-energy transfer processes, as explained in Figure 4 (Frederic et al., 2013). It is shown by the significantly high Stokes's peak power in Figure 6(c) for the narrowest LW pump. When the pump LW is broadened, the Stokes power is reduced as the phase noise dominates.

The obtained OSNR is reduced at around 1 dB when the LW is broadened from 1 kHz to 20 MHz and around ~2.6-dB reduction when the LW is broadened to 50 MHz, equal to the intrinsic Brillouin bandwidth. At 50 MHz pump LW, the obtained BGBW is ~60 MHz for the DSB-SC and SSB-SC/IQ-MZM, while ~40 MHz for the SSB-SC/OBPF. The BGBW will increase proportionally with the increase of pump LW through the relationship between Brillouin LW parameter, Γ and BGBW, Δv_B given by $\Delta v_B \alpha \Gamma \, / \, 2\pi$, where Γ is also related to the pump LW, Δv_p by $\Gamma = f(T_B, \Delta v_B)$ where T_B is phonon lifetime (Zhao et al., 2020). Nevertheless, the results suggest a low-cost distributed feedback laser (DFB) can generate the 50 MHz pump LW. Thus, a low-cost laser source could be used as the pump source.

Figure 7 shows the effect of the pump power on the (a) BG, (b) amplified seed signal power, and (b) amplified seed signal OSNR obtained at Point 4 of Figure 2 using DSB-SC, SSB-SC/OBPF and SSB- SC/IQ-MZM seed generation techniques. The OSNR is obtained using an OSA with respect to 0.1 nm (~12.5 GHz), a typical OSA RBW, and the signal power is measured using a power meter. It is to analyze the SBST for the three designs. The laser time trace is assumed to be stable throughout the loop for Figure 2(a), (b), and (c) without phase mismatch. Figure 7(a) shows that the BG increased linearly with the pump power, and at 10 dBm, it started to increase rapidly. It indicates that a stimulated Brillouin process has taken place, and a pump depletion occurs when the pump power is transferred to the seed signal. It gives the SBST value relatively the same for all three techniques. At the pump power higher than the SBST, most of the power is transferred to the seed signal, resulting in the signal amplification at the Brillouin frequency, v_B, away from f_o and saturating the power of f_o. The BG starts to saturate after 30 dBm of pump power. Figure 7(b) confirms that the f_o power is transferred to the seed signal at $-f_m$ saturates after 30 dBm. Figure 7(c) presents that after 15 dBm peak power, the OSNR of the amplified seed signal using DSB-SC provides a 3-dB better OSNR than the SSB-SC. It confirms the double energy transfer processes between the pump and the USB and LSB of the DSB-SC. The OSNR continues to improve exponentially with the increase of the pump power until at 30

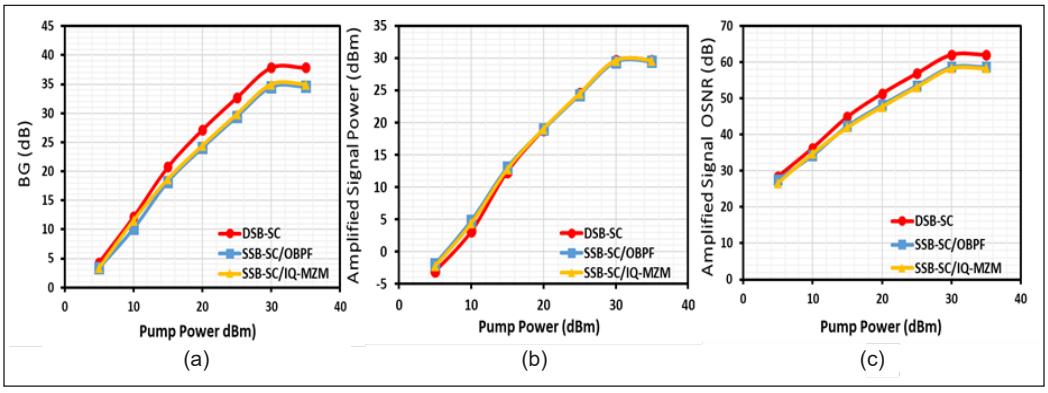

Figure 7. Pump-power effect on (a) BG, (b) amplified signal power, and (c) amplified signal OSNR at Point 4 using DSB-SC, SSB- SC/OBPF and SSB-SC/IQ-MZM seed generation techniques

dBm when it starts to saturate. The highest OSNR obtained is 62.47 dB for the DSB-SC and 58 dB for the SSB-SC. An OSNR enhancement of 37.47 dB is obtained compared to the 25-dB OSNR of the laser source taken at Point 1 of Figure 2 of the DSB-SC.

Figure 8 shows the effect of the MZM biasing voltage concerning the amplified signal OSNR and the seed power. The varying MZM biasing voltages will produce a respective carrier suppression at 193.1 THz laser-pump frequency based on the MZM's transfer function curve and extinction ratio value. The biasing voltages of 0.1 V, 0.5 V, 1 V and 1.6 V produced carrier suppression of 8.1 dB, 20.2 dB, 24.1 dB and 31 dB, respectively. The spectra of Figure 8(a) show that the carrier is suppressed down to the noise floor when the MZM is biased at 1.6 V and a small suppression at 0.1 V. When the carrier is suppressed, the carrier power is distributed to the sidebands or the seed signal at $\pm f_m$ hence producing a high-power seed signal at -6 dBm. When the carrier suppression is small, for example, at 8.1 dB, the power of the seed signal is low at -21 dBm when the MZM is biased at 0.1 V, where a considerably high carrier signal can be seen in the spectrum. High carrier suppression is desired for a coherent transmission system. However, generating the seed signal for an SBS-based amplifier is unnecessary, as shown in Figure 8(b). The lowest carrier suppression of 8.1 dB with its respective seed signal power of -21 dBm of Figure 8(c) provides the best-amplified signal OSNR of ~80 dB. It satisfies the required backward interacting light-wave signal power of tens of microwatts (Du et al., 2023; Marhic & Cholan, 2014; Zan et al., 2013). Moreover, the high carrier in the generated seed signal provides an extended energy transfer between the pump, f_o and $+f_m$ into $-f_m$. When the carrier suppression level is increased, for example, at 20.2 dB, the OSNR of the amplified signal is reduced by close to 14 dB. At a high carrier suppression level of 24.1 dB and 31 dB, when the MZM is biased close to or at the null point of the MZM's transfer function, the produced seed signal power is -2 dBm and -6 dBm, respectively. At this seed signal power, the OSNR becomes saturated. It agreed that the seed signal power should not

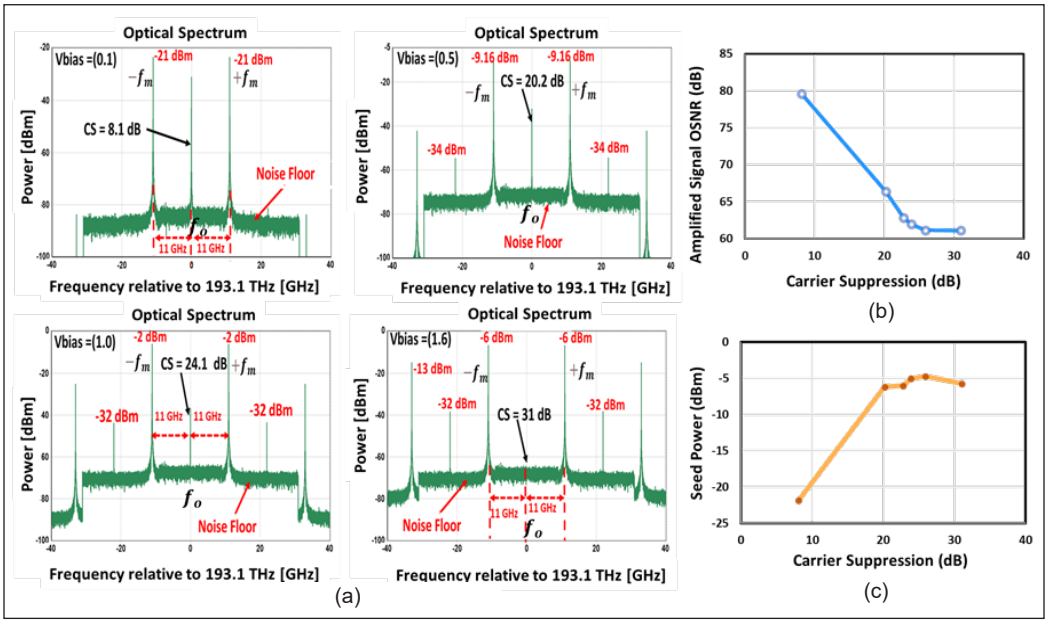

Figure 8. MZM biasing voltage effect with the resulting (a) seed spectra, (b) amplified signal OSNR at Point 4, and (c) seed power at Point 2 using a DSB-SC seed signal generation design

exceed 10 μW to prevent BGS distortion. The high seed signal power will strongly beat within BGBW, and the gain is decreased because the pump-depletion region is prominent at the peak of the BGS.

Furthermore, the carrier suppressed at 24.1 dB and 31 dB will produce high-order harmonics of the carrier and sidebands. It can induce intermodulation distortion between the harmonics and the signal sidebands when this amplifier is used for a transmission system. The obtained results can be used as a guide to tune the optimum biasing point for seed generation with respect to the carrier suppression required. A typical commercially available IQ-MZM requires a biasing point higher than the quadrature to produce the small carrier suppression to meet the seed signal power requirement. Since the carrier suppression is insignificant in producing a high Brillouin gain, a cheap MZM with a low extinction ratio can be used for the seed signal generation. The requirement of SSB-SC/IQ-MZM can be relaxed as DSB-SC without a stringent carrier suppression requirement is shown to perform well. Furthermore, an EDFA to compensate for the insertion loss of the MZM is also not required for the seed generation block.

CONCLUSION

This work investigated the amplification performance of modulation techniques to generate a seed signal using DSB-SC, SSB-SC/OBPF and SSB-SC/IQ-MZM driven by a single CW laser pump using simulation. The three techniques used an MZM to generate the

seed signal at a BFS of 11 GHz, where the SSB is obtained using an OBPF and IQ-MZM. The produced seed will beat within a BGBW to obtain the amplified signal. The OSNR enhancements achieved are 37.47 dB, 33.14 dB and 32.67 dB using DSB-SC, SSB-SC/ OBPF and SSB-SC/IQ-MZM, respectively. It is found that the DSB- SC seed generation modulation technique performed the best with the highest amplified seed signal of 62.47 dB compared to 58.14 dB and 57.67 dB obtained with SSB SC/OBPF and SSBSC/ IQ-MZM. The dual-energy transfer occurs through the beating process involving the USB and LSB instead of the single-energy transfer in the SSB-SCs. Laser pump phase noise represented by the LW is also a limiting factor for the BG as it reduces the gain and induces fluctuations. However, the BG performance tolerates the LW of 50 MHz with a slight OSNR reduction of ~3-dB measured from the resulting amplified seed signal for all generation techniques. It suggests that a low-cost laser source, such as a DFB laser, can be used as a pump source if the OSNR requirement is not critical. Also, the carrier suppression ratio of the resulting DSB and SSB modulation signals is less significant. The seed signal power must be as low as tens of microwatt to prevent the distortion of the BGS and pump depletion. It permits using a low-cost MZM with a low extinction ratio value.

ACKNOWLEDGEMENTS

This work was supported by the Fundamental Research GrantScheme (FRGS), Ministry of Higher Education, Malaysia, No. FRGS/1/2019/TK04/UPM/02/8 and 6300294/UPM/ National Instruments Research Grant.

REFERENCES

Ali, M., Haxha, S., & Flint, I. (2022). Tuneable microwave photonics filter based on stimulated brillouin scattering with enhanced gain and bandwidth control. *Journal of Lightwave Technology, 40*(2), 423-431. https://doi.org/10.1109/JLT.2021.311831

Aoki, Y., Tajima, K., & Mito, I. (1988). Input power limits of single-mode optical fibers due to stimulated Brillouin scattering in optical communication systems. *Journal of Lightwave Technology, 6*(5), 710-719. https://doi.org/10.1109/50.4057

Bhogal, R. K., & Sindhwani, M. (2022). Generation of single sideband-suppressed carrier (SSB-SC) signal based on stimulated brillouin scattering. *Journal of Physics: Conference Series 2327*(1), Article 012025. https://doi.org/10.1088/1742-6596/2327/1/012025

Deventer, M. O. V., & Boot, A. J. (1994). Polarization properties of stimulated Brillouin scattering in single-mode fibers. *Journal of Lightwave Technology*, *12*(4), 585–590. https://doi.org/10.1109/50.285349

Du, S., Liu, X., Du, P., Wang, D., Ma, B., Li, D., Wang, Y., Zhang, J., Wang, Y., & Wang, A. (2023). Broadband microwave photonic frequency measurement based on optical spectrum manipulation and stimulated Brillouin scattering. *IEEE Photonics Journal, 15*(2), Article 5500708. https://doi.org/10.1109/ JPHOT.2023.3251974

Frederic, A., Veronique, Q., Mikael, G., Andre, P., & Yves, A. (2013). A low-consumption electronic system developed for a 10 km long all-optical extension dedicated to sea floor observatories using power-over-fiber technology and SPI protocol. *Microwave and Optical Technology Letters, 55*(11), 2562-2568. https://doi.org/10.1002/mop.27916

Gertler, S., Otterstrom, N. T., Gehl, M., Starbuck, A. L., Dallo, C. M., Pomerene, A. T., Trotter, D. C., Lentine, A. L., & Rakich, P. T. (2022). Narrowband microwave-photonic notch filters using Brillouin-based signal transduction in silicon. *Nature Communications, 13*(1), Article 1947. https://doi.org/10.1038/s41467-022-29590-0

Gökhan, F. S., Göktaş, H., & Sorger, V. J. (2018). Analytical approach of Brillouin amplification over threshold. *Applied Optics, 57*(4), 607-611. https://doi.org/10.1364/AO.57.000607

Harish, A. V., & Nilsson, J. (2019). Suppression of stimulated Brillouin scattering in single-frequency fiber Raman amplifier through pump modulation. *Journal of Lightwave Technology, 37*(13), 3280-3289. https://doi.org/10.1109/JLT.2019.2914081

Loayssa, A., Hernández, R., Benito, D., & Galech, S. (2004). Characterization of stimulated Brillouin scattering spectra by use of optical single-sideband modulation. *Optics Letters, 29*(6), 638-640. https://doi.org/10.1364/OL.29.000638

Mandalawi, Y. N. A., Yaakob, S., Adnan, W. A. W., Yaacob, M. H., & Zan, Z. (2019). Laser phase noise effect and reduction in self-homodyne optical OFDM transmission system. *Optics Letters, 44*(2), 307-310. https://doi.org/10.1364/OL.44.000307

Marhic, M. E., & Cholan, N. A. (2014, June 8-13). *Improvement of optical signal-to-noise ratio of a high-power pump by stimulated brillouin scattering in an optical fiber*. [Paper Presentation]. Conference on Lasers and Electro-Optics (CLEO), San Jose, USA. https://doi.org/ 10.1364/CLEO_SI.2014.SM4N.6

Nieves, O. A., Arnold, M. D., Steel, M. J., Schmidt, M. K., & Poulton, C. G. (2021). Noise and pulse dynamics in backward stimulated Brillouin scattering. *Optics Express, 29*(3), 3132-3146. https://doi.org/10.1364/OE.414420

Pan, J., Richter, T., & Tibuleac, S. (2018, March 11-15). *OSNR Measurement comparison in systems with ROADM filtering for flexible grid networks.*[Paper presentation]. Optical Fiber Communications Conference and Exposition (OFC), San Diego, California.

Pang, Y., Xu, Y., Zhao, X., Qin, Z. & Liu, Z. (2022). Stabilized narrow-linewidth brillouin random fiber laser with a double-coupler fiber ring resonator. *Journal of Lightwave Technology*, *40*(9), 2988–2995. https://doi.org/10.1109/jlt.2022.3148118

Preussler, S., & Schneider, T. (2016). Stimulated Brillouin scattering gain bandwidth reduction and applications in microwave photonics and optical signal processing. *Optical Engineering, 55*(3), Article 031110. https://doi.org/10.1117/1.OE.55.3.031110

Qi, T., Li, D., Wang, Z., Wang, L., Yu, W., Yan, P., Gong, M., & Xiao, Q., (2022). 6.85 KW ytterbium-raman fiber amplifier based on adjustable raman threshold method. *Journal of Lightwave Technology, 40*(12), 3907-3915. https://doi.org/10.1109/JLT.2022.3151489

Qing, T., Li, S., Xue, M., & Pan, S. (2016). Optical vector analysis based on double-sideband modulation and stimulated Brillouin scattering. *Optics Letters, 41*(15), 3671-3674. https://doi.org/10.1364/OL.41.003671

Ravet, F., Snoddy, J., Bao, X., & Chen, L. (2008). Power thresholds and pump depletion in Brillouin fiber amplifiers. *The Open Optics Journal, 2*(1), 1-5. https://doi.org/10.2174/1874328500802010001

Souidi, Y., Taleb, F., Zheng, J., Lee, M. W., Du Burck, F., & Roncin, V. (2016). Low-noise and high-gain Brillouin optical amplifier for narrowband active optical filtering based on a pump-to-signal optoelectronic tracking. *Applied Optics, 55*(2), 248–253. https://doi.org/10.1364/AO.55.000248

Zan, M. S. D. B., Tsumuraya, T., & Horiguchi, T. (2013). The use of Walsh code in modulating the pump light of high spatial resolution phase-shift-pulse Brillouin optical time domain analysis with non-return-to-zero pulses. *Measurement Science and Technology, 24*(9), Article 094025. https://doi.org/10.1088/0957-0233/24/9/094025

Zhang, Q., Han, X., Shao, X., Wang, Y., Jiang, H., Dong, W., & Zhang, X. (2022). Stimulated Brillouin scattering-based microwave photonic filter with a narrow and high selective passband. *IEEE Photonics Journal*, *14*(4), Article 5537507. https://doi.org/10.1109/JPHOT.2022.3184761

Zhao, J., Yang, F., Wei, F., Zhang, X., Ding, Z., Wu, R., & Cai, H. (2020). Effect of linewidth on intensity noise induced by stimulated Brillouin scattering in single-mode fibers. *Optics Express, 28*(10), 15025–15034. https://doi.org/10.1364/OE.393239